

# Impedance spectroscopy study of the AC conductivity of sodium superoxide nanoparticles doped vanadate based glasses

R.V. Barde<sup>a,\*</sup>, K.R. Nemade<sup>b</sup>, S.A. Waghuley<sup>c</sup>

<sup>a</sup> Department of Physics, Govt. Vidarbha Institute of Science and Humanities, Amravati, India

<sup>b</sup> Department of Physics, Indira Mahavidyalaya, Kalamb, India

<sup>c</sup> Department of Physics, Sant Gadge Baba Amravati University, Amravati, India

## ARTICLE INFO

### Article history:

Received 25 April 2021

Revised 17 June 2021

Accepted 19 June 2021

Available online 24 June 2021

### Keywords:

Sodium superoxide

Nyquist plots

Electrical conductivity

Impedance spectroscopy

Hopping distance

## ABSTRACT

In the present work, we successfully prepared sodium superoxide (NaO<sub>2</sub>) doped vanadium phosphate borate glasses using normal melt quenching technique of composition 60V<sub>2</sub>O<sub>5</sub>–5P<sub>2</sub>O<sub>5</sub>–(35–x) B<sub>2</sub>O<sub>3</sub>–xNaO<sub>2</sub>, x = 0, 10, 15 and 20 mol %. The foremost objective of this work is to explore the transport properties of sodium superoxide doped vanadium phosphate borate glasses. The impedance spectroscopy was employed to investigate transport properties of all glass systems under study. The AC conductivity for all glass systems were investigated in temperature range 308–473 K. The Jonscher's power law found to be fit with conductivity data, which decrease with temperature and satisfies the criteria of the correlated hopping model. The activation energy (E<sub>a</sub>) estimated from the Arrhenius plot and it is observed to be 0.12 eV.

© 2021 The Authors. Publishing services by Elsevier B.V. on behalf of KeAi Communications Co. Ltd. This is an open access article under the CC BY-NC-ND license (<http://creativecommons.org/licenses/by-nc-nd/4.0/>).

## 1. Introduction

Conducting glasses with superionic electrochemistry are potential candidate for solid state batteries due their excellent conductivity and chemical stability against atmospheric changes. In this category of conducting glasses, V<sub>2</sub>O<sub>5</sub> glasses has an inordinate potential due to its practical advantages like generating various structural groups [1], providing wide range of structure [2], showing optical as well as electrical properties and mainly its capability as a host for different metallic ions [3]. These properties generally used in fabrication of electrochemical batteries [4], memory switching devices [5] and supercapacitor [6]. The electrical properties of glasses containing large amount of transition metal oxide such as V<sub>2</sub>O<sub>5</sub> are determine by the transition metal ions present in two different valence states V<sup>4+</sup> and V<sup>5+</sup> [7]. The conduction mechanism in such glasses is dominated by small polaron hopping amongst such ions [8].

Since long time, much attention is attracted by B<sub>2</sub>O<sub>3</sub>–P<sub>2</sub>O<sub>5</sub> glasses for their low refractive index and extraordinary optical properties [9]. These glasses show excellent chemical durability when doped with transition metals than that of phosphate glasses due to boron oxide in the glass network in the form of BO<sub>4</sub> tetrahedral and it transforms metaphosphate chain into 3D network [10]

which useful as tuneable solid-state lasers [11], optical [12] and luminescence materials [13], memory devices [14], solar energy converters [15] and fiber optic communication devices [16].

The better formation of NaO<sub>2</sub> at the oxygen side is mainly due to the transport limitation of gaseous oxygen through the electrolyte-filled cathode structure. It is recognized that, NaO<sub>2</sub> can be formed as a stable and solid compound which is the discharge product in a NaO<sub>2</sub> cell with a diglyme based electrolyte and it provides easier access to the study of the cell chemistry as compared to LiO<sub>2</sub> cells, because discharge products are easily noticeable due to the stronger interaction of sodium with spectroscopic probes [17].

For researchers it is very difficult task to prepared stable superoxide. The spray pyrolysis technique is employed for preparation of sodium superoxide nanoparticles in which oxygen rich environment is maintain to achieve higher degree of purity in superoxide phase [18]. As discussed earlier, preparation of stable NaO<sub>2</sub> is the key barrier in the realization of sodium-air batteries. This instability is attributed to discharge product of sodium superoxide is reversibly oxidized toward oxygen as compared to peroxide and oxide [19]. The rechargeable room-temperature battery application of NaO<sub>2</sub> was demonstrated by Hartmann et al. The results of the study show that sodium superoxide crystals forms as a solid discharge in a one-electron transfer step. This work opens the possibility of the substitution of Li-ion batteries by sodium, which offers an unexpected result as metal–air batteries [20].

\* Corresponding author.

E-mail address: [rajeshbarde1976@gmail.com](mailto:rajeshbarde1976@gmail.com) (R.V. Barde).

Some recent reports suggest that vanadates glass system is appropriate for high temperature battery applications. Khan et al reported the Li doped vanadates glass system useful for battery/solid oxide fuel cell due to their good conductivity. The results of the study shows that DC conductivity of the present samples is increased from 0.08 to 0.12  $\text{Scm}^{-1}$  at 450 °C with  $\text{Li}_2\text{O}$  doping. Also, the optical band gap decreases from 2.2 to 2.08 eV and Urbach energy increases from 0.31 to 0.41 eV with the addition of  $\text{Li}_2\text{O}$ . These aspects make Li doped vanadates system useful for battery application at higher temperature [21].

Hailemariam et al studied the impedance spectroscopic of lithium substituted niobo vanadate glasses using Nyquist plots and electrical conductivity analysis. In this work, the DC part of the electrical conductivity was studied using alkali ion distance and alkali-oxygen distance method. The activation energy shows the variation with lithium content, it decreases from 0.54 to 0.39 eV as lithium content increases. The mobility study of lithium ions depicts that the decrease in lithium content increases mobility [22].

Alves et al reported the bismuth-vanadate glass system based a novel photochemiresistor sensor for the determination of chemical oxygen demand. The thin film of bismuth-vanadate glass system shows the monoclinic phase deposited on an FTO glass surface. The thin film works efficiently and shows a good correlation between the charge transfer resistance and chemical oxygen demand concentration in the electrolyte solution [23].

Sujatha et al reported the microwave based novel approach for the preparation of Li-vanadate based glasses. This study concludes that microwave-based preparation approach offers advantage of efficient transformation of energy throughout the volume in an effectively short time. Impedance and electron paramagnetic resonance spectroscopic studies of as prepared Li-vanadate based glass system shows the explicate the nature of conduction mechanism [24].

Inspiring from above discussion and research gap identified from literature of materials science, we plan to report first time the transport properties of sodium superoxide loaded vanadate glasses. The main accomplishment of present work is that we successfully prepared the superoxide based stable glasses for transport properties measurement. Typically, the study of conducting glass comprising parameters like frequency exponent and scaling to modulus. The purpose of this work is to analyse the effect of  $\text{NaO}_2$  addition in glasses on temperature and frequency of the polarization by means of electrical conductivity, dielectric constant and modulus in the frequency and temperature range 20 Hz to 1 MHz and 308 to 473 K respectively. The structural, physical and topographical study of prepared glass samples were completed using X-ray diffraction (XRD).

## 2. Experimental

### 2.1. Materials

$\text{NaO}_2$  was prepared by using AR grade sodium nitrate (SD fine). Glass samples were prepared by using vanadium pentoxide ( $\text{V}_2\text{O}_5$ ), phosphorus pentoxide ( $\text{P}_2\text{O}_5$ ) and boric acid ( $\text{H}_3\text{BO}_3$ ) along with a prepared  $\text{NaO}_2$ .

### 2.2. Preparation of $\text{NaO}_2$ and glass samples

For the present work, sodium superoxide ( $\text{NaO}_2$ ) was prepared using spray pyrolysis executed with oxygen rich environment at temperature 673 K. The sodium nitrate and hydrogen peroxide were used as precursors for the preparation of  $\text{NaO}_2$ . The suspension for spray pyrolysis was prepared by adding 1 M of sodium

nitrate in 20 ml  $\text{H}_2\text{O}$  under strong magnetic stirring. Subsequently, this suspension was employed for spraying under constant oxygen flow on  $\text{SiO}_2$  heating substrate. Its phase purity and structure of as-prepared  $\text{NaO}_2$  was confirmed through XRD study. The usual melt-quenching method was used for the preparation of glass samples of compositions  $60\text{V}_2\text{O}_5-5\text{P}_2\text{O}_5-(35-x)\text{B}_2\text{O}_3-x\text{NaO}_2$ ,  $x = 0, 10, 15$  and 20 mol %. They were weighed and mixed together. This mixture was homogenized and melted in silica crucible in a furnace at 900 °C for 3 h. After melting, the mixture was poured out onto a nonmagnetic stainless-steel plate maintained at temperature 15 °C and pressed with another stainless-steel substrate so that the sheet sample had a circular shape and a thickness of about 4 mm. To avoid internal strains, the sample was annealed at 200 °C for 1 h and then cooled slowly to room temperature. [25–27]. The melts were three times stirred during heating to attain homogeneous glasses and lastly poured on an aluminum plate and pressed immediately by another aluminum plate.

### 2.3. Characterizations

The powder samples were characterized at room temperature by using Bruker D8 advance with  $\text{Cu K}\alpha$  radiation with scan rate 6.00 in the range 10°–80° to study morphologies of all samples.

### 2.4. Impedance study

The LCR meter, Agilent Technology, Singapore was used for impedance study which directly gives the impedance ( $Z$ ), phase angle ( $\theta$ ), capacitance ( $C$ ) and the resistance ( $R$ ) in a frequency and temperature region of 20 Hz to 1 MHz and 308–473 K respectively. For these measurements, the samples were cut into circular discs, polished and conducting silver paste was deposited on both sides. The sample area was taken to be the area exposed to the electrode surface. A firm contact was confirmed at the boundaries of the sample/electrode interfaces. By using above parameter AC conductivity was obtained. From the  $Z$  and  $\theta$  data the values of  $Z'$  and  $Z''$  computed from  $|Z| \cos \theta$  and  $|Z| \sin \theta$ , respectively. The results presented in this work are average of three trials of reading to avoid errors measurement. During trials no significant deviation was observed in reading.

## 3. Result and discussion

### 3.1. XRD analysis

XRD pattern of sodium superoxide ( $\text{NaO}_2$ ) is shown in Fig. 1 (i). The four peaks positions (200), (220), (311) and (222) appear in pattern exactly index to  $\text{NaO}_2$  according to JCPDS reference card No. 01-077-0207, which confirms the formation of  $\text{NaO}_2$  [17]. XRD pattern of prepared samples (Fig. 1(ii)), confirms the formation of glasses (amorphous nature), as there was no distinguishing peak corresponds to any crystalline phase. [26].

### 3.2. Impedance study

The experimental impedance data for 20 mol % of  $\text{NaO}_2$  glass sample at different temperatures as Nyquist plots is shown in Fig. 2 (a), (b) and (c). It is observed that, with increase in temperature, the inclined straight line disappears with the formation of semicircle. It is observed that, the center of completely formed depressed semicircle and partially formed semicircle is positioned below the real impedance axis, which reveals a non-Debye relaxation behavior with distributed relaxation time and the intercept of semicircle with the real axis shift towards lower frequency at distinct temperature. At higher temperatures this intercept shifted

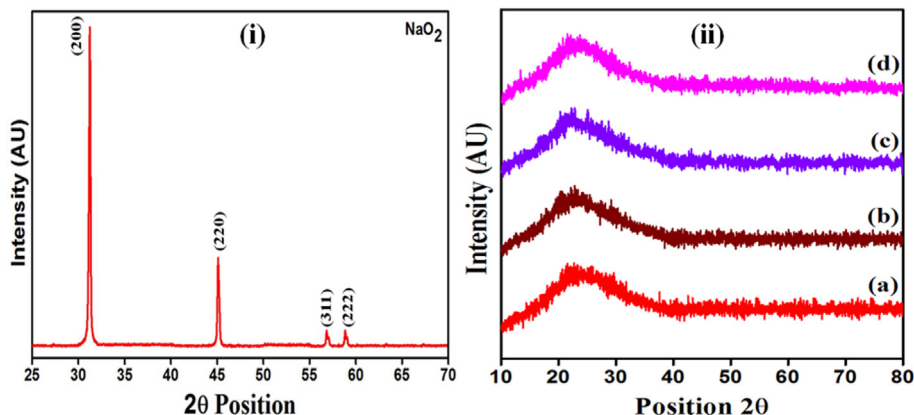


Fig. 1. (i) XRD of Sodium Superoxide (NaO<sub>2</sub>) and (ii) XRD of 60V<sub>2</sub>O<sub>5</sub>-5P<sub>2</sub>O<sub>5</sub>-(35-x)B<sub>2</sub>O<sub>3</sub>-xNaO<sub>2</sub> for (a) 0 mol%, (b) 10 mol%, (c) 15 mol% and (d) 20 mol% of NaO<sub>2</sub>.

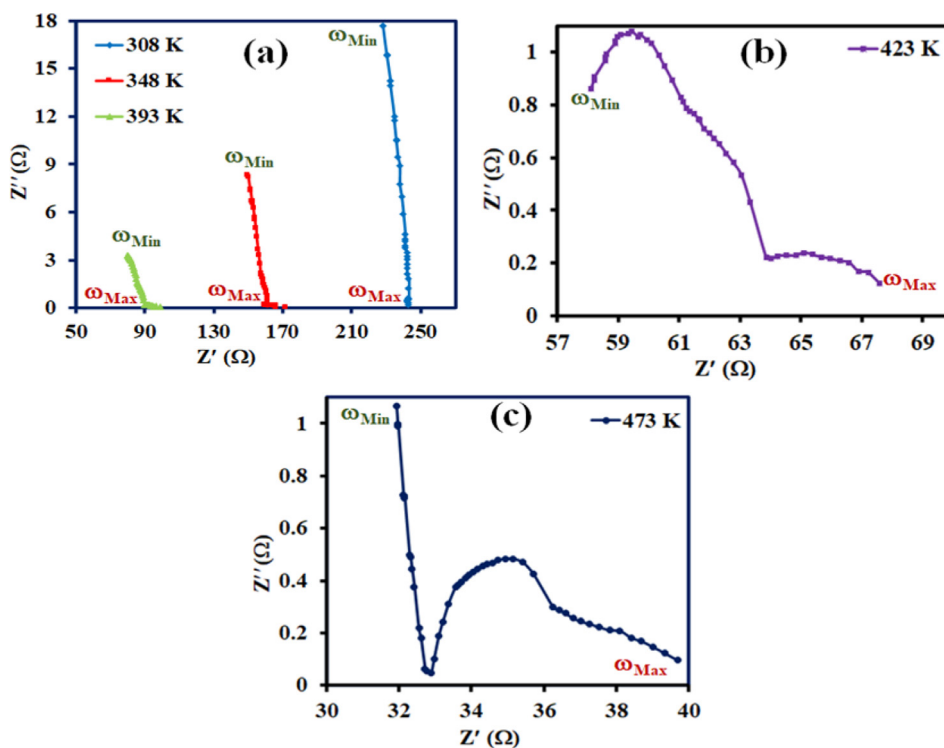


Fig. 2. Nyquist plots of 20 mol % of NaO<sub>2</sub> at different temperature.

towards origin and it gives the bulk resistance of the sample at various temperatures. In these glasses, the electrical relaxation is purely a bulk phenomenon which is mainly due to the absence of a low frequency electrode spike [28, 29]. The double layer capacitance of these glasses confirms from the equivalent circuit of dejected semicircle which is the parallel combination of bulk resistance and constant phase element (CPE). The similar behaviour is also observing for other glass samples. From the intercepts of the semicircle of low frequency with real impedance axis, the DC conductivity ( $\sigma_{dc}$ ) is calculated using sample dimensions at various temperatures [30]. Its value thus shows a gradual enhancement with the increase in temperature that is with the increase in temperature, bulk resistance of the sample decreases, which is activated conduction mechanism. The dc conductivity plot shown in Fig. 3 fitted to Arrhenius equation

The activation energy,  $E_{dc}$  was calculated from the least square straight-line fitting of plot. The lowest value of activation energy was found to be 0.12 eV for 20 mol % of NaO<sub>2</sub>. It is observed that

conductivity increases with increase in mol % of NaO<sub>2</sub>. The maximum in conductivity corresponds with minimum of activation energy. The explanation for enhancement in conductivity is given on the basis of the Anderson and Stuart model. According to this model, as one of the glass former ion is substituted by another glass former ion, the average interionic bond distance changes. It becomes larger/smaller depending on substituting ion is larger/smaller. Thus, with the addition of NaO<sub>2</sub> content, the structure becomes loose and hence conductivity increases [31–33].

### 3.3. AC conductivity

The frequency dependence of AC conductivity for 20 mol % of NaO<sub>2</sub> glass sample at different temperatures is shown in Fig. 4. These figures shows that AC conductivity increases linearly with frequency. The temperature dependence of AC conductivity in glasses is studied in the glass transition regime. From Fig. 4, suggest two thermally activated phenomena for conduction i.e. this

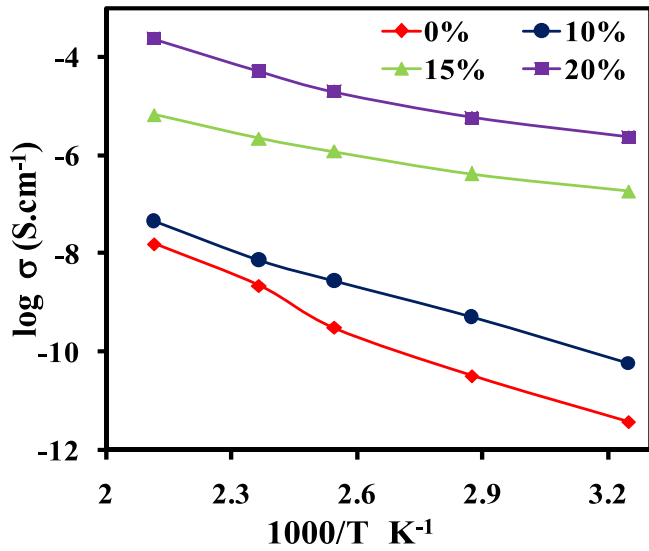


Fig. 3. dc conductivity Plot of all glass samples with varying temperature.

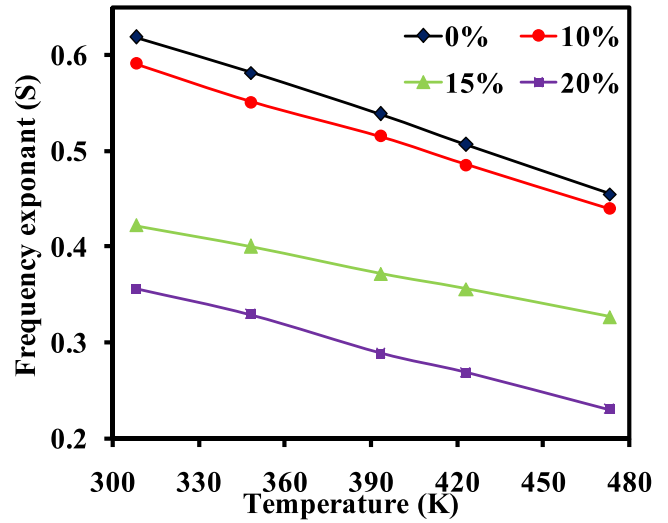


Fig. 5. Variation of frequency exponent (s) with temperature for all samples.

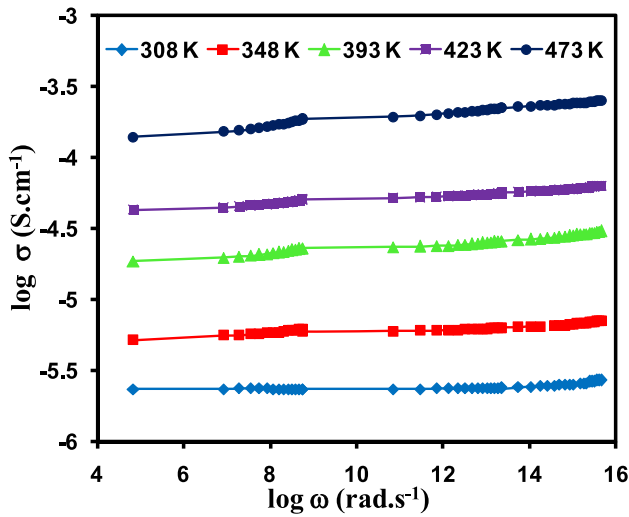


Fig. 4. Variation of Conductivity of 20 mol % Na<sub>2</sub>O<sub>2</sub> of with temperature.

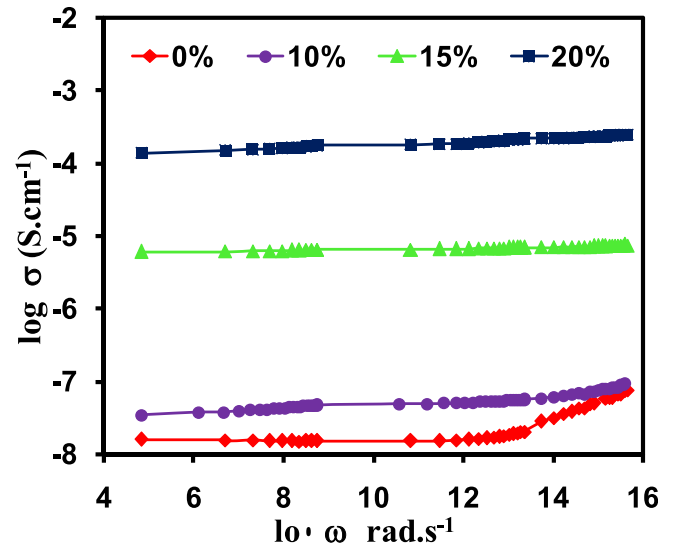


Fig. 6. Variation of Conductivity with mol % of Na<sub>2</sub>O in temperature range 308 – 473 K.

plot consists of two distinct regions low frequency plateau region and high frequency dispersion region. In plateau region the conductivity is observed to be almost independent of frequency suggesting that the ionic diffusion is random less via activated hopping process and by extrapolating the conductivity value to zero limit frequency the dc conductivity obtained which shows good agreement with the dc conductivity obtained from impedance plot indicating the thermally induced process due to the increase in the energy of charge carriers [34]. In high frequency region dispersion is predominant at low temperature and becomes prominent with increase in temperature (linear behavior) and it shift to higher frequency region, which was analysed by Jonscher's Universal Power law [35,36]. Comparable nature is also observed in other glasses.

$$\sigma(\omega) = \sigma(0) + A\omega^s \quad (2)$$

$\sigma(0)$  is the direct current conductivity of the sample,  $A\omega^s$  is the pure dispersive component of AC conductivity having a characteristic of power law in terms of angular frequency  $\omega$  and exponent  $S$  ( $0 \leq S \leq 1$ ) that represents the degree of interaction between

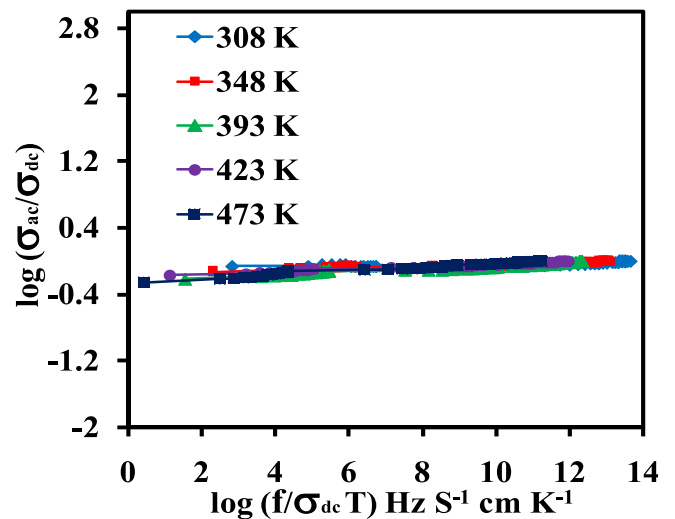


Fig. 7. Conductivity scaling data of 20 mol% Na<sub>2</sub>O glass sample with different temperatures.

**Table 1**  
Activation energy ( $E_a$ ), Frequency exponent ( $s$ ) and Hopping distance ( $R$ ).

Sample mol %	$E_a$ (eV)	Frequency exponent ( $s$ )					Hopping distance ( $R$ )				
		308 K	348 K	393 K	423 K	473 K	308 K	348 K	393 K	423 K	473 K
0	0.28	0.62	0.58	0.54	0.51	0.46	0.42	0.43	0.44	0.44	0.45
10	0.21	0.60	0.55	0.52	0.49	0.44	0.39	0.40	0.42	0.42	0.44
15	0.15	0.42	0.40	0.37	0.36	0.33	0.28	0.30	0.32	0.34	0.36
20	0.12	0.36	0.33	0.29	0.27	0.22	0.25	0.27	0.29	0.30	0.32

mobile ions and the lattices around them, and  $A$  is a constant which determines the strength of polarizability. It is clear that conductivity is dependent on  $\omega^s$  in high frequency regime. The frequency exponent ( $S$ ) lies in between 0.3 and 0.6. The temperature dependence of the frequency exponent, for the investigated glass samples is shown in Fig. 5 [37,38].

It is notable that, from the temperature dependent behaviour of  $s$ , the conduction mechanism in any material can be explained. From figure it is clear that, correlated barrier hopping (CBH) conduction mechanism is predominant for all glasses as,  $s$  decreases with increase in temperature [29]. With the addition of  $\text{NaO}_2$  the transition probability in between valance state  $V^{5+}$  and  $V^{6+}$  increases, which results in enhancement of conductivity.

From Fig. 6 it is observed that, conductivity increases with increasing frequency and mol % of  $\text{NaO}_2$  in the temperature range 308 to 473 K. The result of normalised plot of conduction at different temperature is shown in Fig. 7. It is observed that data for different temperature overlap on single curve which indicates that, conduction mechanism is independent of temperature i.e. dynamic processes occurring at various frequencies needs nearly the same thermal activation energy. [39,40].

The maximum barrier height ( $R$ ) was calculated by using Eq. (3) as [41,42]:

$$R = \frac{6kT}{1-s} \quad (3)$$

where  $k$  is the Boltzmann constant, and  $T$  is the absolute temperature. The values of  $R$  for all samples were listed in Table 1. The maximum barrier height ( $R$ ) increases with temperature whereas decreases with increasing  $\text{NaO}_2$  content as shown in Fig. 8.

The comparison of results of this work with recent works reported by Khan et al [21] and Hailemariam et al [22], our  $\text{NaO}_2$ -vanadate based glass system shows good and stable Impedance and AC conductivity properties.

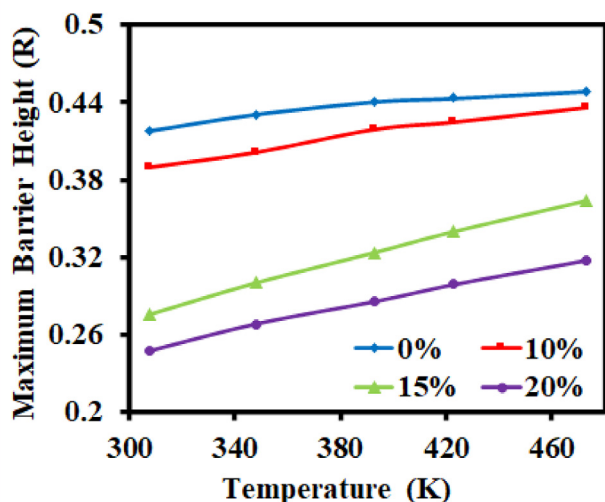


**Fig. 8.** Variation of maximum barrier height ( $R$ ) with temperature for all samples.

## 4. Conclusions

The formation of  $\text{NaO}_2$  was confirmed by using XRD analysis. Similarly, the amorphous nature of all glass systems was confirmed from XRD analysis. The addition of  $\text{NaO}_2$  increases significantly the conductivity of glasses. In the summary of present work, it is concluded that sodium superoxide is a potential dopant to improve transport characteristics of conducting glasses. The universal power law was employed to investigate variation of AC conductivity. Results shows that temperature increases and frequency exponent ( $s$ ) decreases during AC conduction. The results of the study found fit with Elliot's correlated barrier hopping model (CBH). The scaling study confirms that conduction mechanism shows direct dependency on composition of glass system and temperature independent.

In summary, we first time successfully explored the impedance spectroscopy and AC conductivity study of sodium superoxide nanoparticles doped vanadates-based glasses. The major accomplishment of present study is that we succeed in preparation of stable superoxide-based glasses, which shows good transport characteristics over the wide range of temperature. This virtue make glass useful for wide variety of applications such as high temperature battery application, supercapacitor application.

## Declaration of Competing Interest

The authors declare that they have no known competing financial interests or personal relationships that could have appeared to influence the work reported in this paper.

## Acknowledgements

Authors are thankful to Head Department of physics, Director, Government Vidarbha Institute of Science and Humanities, Amravati and Head, Department of Physics Sant Gadge Baba Amravati University, Amravati for providing necessary facilities.

## References

- [1] G.I. Petrov, V.V. Yakovlev, J. Squier, Raman microscopy analysis of phase transformation mechanisms in vanadium dioxide, *Appl. Phys. Lett.* 81 (6) (2002) 1023–1025.
- [2] M.M. El-Desoky, M.S. Al-Assiri, Structural and Polaronic transport properties of semiconducting  $\text{CuO-V}_2\text{O}_5\text{-TeO}$  glasses, *Mater. Sci. Eng. B* 137 (2007) 237–246.
- [3] G.M. Clark, A.N. Pick, DTA study of the reactions of  $\text{V}_2\text{O}_5$  with metal (II) oxides, *J. Therm. Anal.* 7 (2) (1975) 289–300.
- [4] H. Liu, D. Tang, Synthesis of  $\text{ZnV}_2\text{O}_6$  powder and its cathodic performance for lithium secondary battery, *Mater. Chem. Phys.* 114 (2-3) (2009) 656–659.
- [5] E. Mansour, Y.M. Moustafa, G.M. El-Damrawi, S. Abd El-Maksoud, H. Doweidar, Memory switching of  $\text{Fe}_2\text{O}_3\text{-BaO-V}_2\text{O}_5$  glasses, *Physica B* 305 (2001) 242–249.
- [6] K. Jeyalakshmi, S. Vijayakumar, S. Nagamuthu, G. Muralidharan, Effect of annealing temperature on the supercapacitor behaviour of  $\beta\text{-V}_2\text{O}_5$  thin films, *Mater. Res. Bull.* 48 (2) (2013) 760–766.
- [7] L. Murawski, Electrical conductivity in iron-containing oxide glasses, *J. Mater. Sci.* 17 (1982) 2155–2163.
- [8] N.F. Mott, Conduction in glasses containing transition metal ions, *J. Non-Cryst. Solids* 1 (1) (1968) 1–17.
- [9] S. Yusub, D. Krishna Rao, The role of chromium ions on dielectric and spectroscopic properties of  $\text{Li}_2\text{O-PbO-B}_2\text{O}_3\text{-P}_2\text{O}_5$  glasses, *J. Non-Cryst. Solids* 398–399 (2014) 1–9.

- [10] R.K. Brow, D.R. Tallant, Structural design of sealing glasses, *J. Non-Cryst. Solids* 222 (1997) 396–406.
- [11] T.O. Hardwell, *Solid-state lasers: properties and applications*, Nova Science (2008).
- [12] B. Denker, B. Galagan, V. Osiko, S. Sverchikov, E. Dianov, Luminescent properties of Bi-doped boro-alumino-phosphate glasses, *App. Phys. B* 87 (2007) 135–137.
- [13] C.R. Kesavulu, R.P.S. Chakradhar, R.S. Muralidhara, J. Lakshmana Rao, R.V. Anavekar, EPR, optical absorption and photoluminescence properties of  $\text{Cr}^{3+}$  ions in lithium borophosphate glasses, *J. Alloys Compd.* 496 (2010) 75–80.
- [14] O. Mao, R.L. Turner, I.A. Courtney, B.D. Fredericksen, M.I. Buckett, L.J. Krause, J. R. Dahn, Active/inactive nanocomposites as anodes for Li-ion batteries, *Electrochem. Solid-State Lett.* 2 (1) (1999) 3–5.
- [15] J.T. Tsai, C.Y. Huang, S.T. Lin, The development of conductive pastes for solar cells, *Adv. Mater. Res.* 557–559 (2012) 1201–1204.
- [16] J.W. Yu, K. Oh, New in-line fiber band pass filters using high silica dispersive optical fibers, *Optics Commu.* 204 (1-6) (2002) 111–118.
- [17] Pascal Hartmann, Conrad L. Bender, Joachim Sann, Anna Katharina Dürr, Martin Jansen, Jürgen Janek, Philipp Adelhelm, A comprehensive study on the cell chemistry of the sodium superoxide ( $\text{NaO}_2$ ) battery, *Phys. Chem. Chem. Phys.* 15 (28) (2013) 11661, <https://doi.org/10.1039/c3cp50930c>.
- [18] Kailash Nemade, Sandeep Waghuley, Novel synthesis approach for stable sodium superoxide ( $\text{NaO}_2$ ) nanoparticles for LPG sensing application, *Int. Nano Lett.* 7 (3) (2017) 233–236.
- [19] V.S. Dilimon, C. Hwang, Y. Cho, J. Yang, H. Lim, K. Kang, S.J. Kang, H. Song, Superoxide stability for reversible  $\text{Na-O}_2$  electrochemistry, *Sci. Rep.* 7 (2017) 17635–17642.
- [20] Pascal Hartmann, Conrad L. Bender, Miloš Vračar, Anna Katharina Dürr, Arnd Garsuch, Jürgen Janek, Philipp Adelhelm, A rechargeable room-temperature sodium superoxide ( $\text{NaO}_2$ ) battery, *Natu. Mater.* 12 (3) (2013) 228–232.
- [21] S. Khan, K. Singh, Structural, optical, thermal and conducting properties of  $\text{V}_2\text{-xLi}_x\text{O}_5\text{-}\delta$  ( $0.15 \leq x \leq 0.30$ ) systems, *Sci. Rep.* 10 (2020) 1–11.
- [22] B.G. Hailemariam, G.V. Honnavar, M. Irfan, R. Keralapura, Structural and electrical properties of lithium substituted niobo vanadate glasses doped with nickel ferrite, *AIP Adv.* 11 (2021) 210–220.
- [23] N.A. Alves, A. Olean-Oliveira, C.X. Cardoso, M.F.S. Teixeira, Photochemiresistor sensor development based on a bismuth vanadate type semiconductor for determination of chemical oxygen demand, *ACS Appl. Mater. Interfaces* 12 (2020) 18723–18729.
- [24] Basareddy Sujatha, Ramarao Viswanatha, Hanumathappa Nagabushana, Chinnappa Narayana Reddy, Electronic and ionic conductivity studies on microwave synthesized glasses containing transition metal ions, *J. Mater. Res. Technol.* 6 (1) (2017) 7–12.
- [25] R.V. Barde, S.A. Waghuley, Preparation and electrical conductivity of novel vanadate borate glass system containing graphene oxide, *J. Non-Cryst. Solids* 376 (2013) 117–125.
- [26] Rajesh Barde, Sandeep Waghuley, Transport properties of rare earth  $\text{CeO}_2$  doped phospho-vanadate glass systems, *J. Chin. Adv. Mater. Soc.* 2 (4) (2014) 273–283.
- [27] A. V. Sekhar, L. Pavic, A. Mogus-Milankovic, V. R. Kumar, A. S. Sessa Reddy, G. N. Raju, and N. Veeraiah, Dielectric dispersion and impedance spectroscopy of NiO doped  $\text{Li}_2\text{SO}_4\text{MgOeP}_2\text{O}_5$  glass system, *J. of Allo. and Comp.*, 824 (2020) 153907.
- [28] S. Jayaseelan, P. Muralidharan, M. Venkateshwarlu, N. Satyanarayana, Ion transport and relaxation studies of silver vanado tellurite glasses at low temperature, *Mate. Chem. and phys.* 87 (2004) 370–377.
- [29] Saroj Rani, Sujata Sanghi, Neetu Ahlawat, Ashish Agarwal, Influence of  $\text{Bi}_2\text{O}_3$  on physical, electrical and thermal properties of  $\text{Li}_2\text{O-ZnO-Bi}_2\text{O}_3\text{-SiO}_2$  glasses, *J. Alloys Comp.* 619 (2015) 659–666.
- [30] R.V. Barde, S.A. Waghuley, Study of AC electrical properties of  $\text{V}_2\text{O}_5\text{-P}_2\text{O}_5\text{-B}_2\text{O}_3\text{-Dy}_2\text{O}_3\text{-xCeO}_2$  glasses, *Ceram. Inter.* 39 (6) (2013) 6303–6311.
- [31] C.R. Mariappan, G. Govindaraj, S. Vinoth Rathan, G. Vijaya Prakash, Preparation, characterization, AC conductivity and permittivity studies on vitreous  $\text{M}_4\text{AlCdP}_3\text{O}_{12}$  ( $\text{M} = \text{Li, Na, K}$ ) system, *Mater. Sci. Eng. B* 121 (1-2) (2005) 2–8.
- [32] R.S. Gedam, V.K. Deshpande, An anomalous enhancement in the electrical conductivity of  $\text{Li}_2\text{O} : \text{B}_2\text{O}_3 : \text{Al}_2\text{O}_3$  glasses, *Solid State Ionics* 177 (26-32) (2006) 2589–2592.
- [33] R.V. Barde, S.A. Waghuley, Thermal and electrical properties of  $60\text{V}_2\text{O}_5\text{-}5\text{P}_2\text{O}_5\text{-}(35\text{-x})\text{B}_2\text{O}_3\text{-xCeO}_2$  ( $1 \leq x \leq 5$ ) glasses, *Bull. Mater. Sci.* 38 (2) (2015) 557–563.
- [34] P. Jaiswal, P.K. Singh, P. Lohia, D.K. Dwivedi, Study of ac conductivity mechanism and impedance spectroscopy in CNT-added  $\text{Cu}_5\text{Se}_7\text{Te}_{10}\text{In}_{10}$  chalcogenide system, *Bull. Mater. Sci.* 43 (2020) 216.
- [35] B. Saravanakumar, G. Ravi, V. Ganesh, R.K. Guduru, R. Yuvakkumar,  $\text{MnCo}_2\text{O}_4$  nanosphere synthesis for electrochemical application, *Mater. Sci. Ener. Techn.* 2 (2019) 130–138.
- [36] P.M. Anjana, M.R. Bindhu, R.B. Rakhi, Green synthesized gold nanoparticle dispersed porous carbon composites for electrochemical energy storage, *Mater. Sci. for Ene. Tech.* 2 (3) (2019) 389–395.
- [37] C. Dohare, M.M.A. Imran, N. Mehta, Study of dielectric relaxation and thermally activated a.c. conduction in glassy  $\text{Se}_{70}\text{Te}_{30}$  and  $\text{Se}_{70}\text{Te}_{28}\text{M}_2$  ( $\text{M} = \text{Ag, Zn and Cd}$ ) alloys, *J. Asi. Ceram. Soc.* 4 (2016) 252–258.
- [38] Ah Dhahri, E. Dhahri, E.K. Hlil, Electrical conductivity and dielectric behaviour of nanocrystalline  $\text{La}_{0.6}\text{Gd}_{0.1}\text{Sr}_{0.3}\text{Mn}_{0.75}\text{Si}_{0.25}\text{O}_3$ , *RSC Adv.* 8 (17) (2018) 9103–9111.
- [39] B. Roling, A. Happe, K. Funke, M.D. Ingram, Carrier concentrations and relaxation spectroscopy: new information from scaling properties of conductivity spectra in ionically conducting glasses, *Phys. Rev. Lett.* 78 (11) (1997) 2160–2163.
- [40] Somyia El-Sayed, Optical properties and dielectric relaxation of polyvinylidene fluoride thin films doped with gadolinium chloride, *Physica B* 454 (2014) 197–203.
- [41] R.V. Barde, K.R. Nemade, S.A. Waghuley, AC conductivity and dielectric relaxation in  $\text{V}_2\text{O}_5\text{-P}_2\text{O}_5\text{-B}_2\text{O}_3$  glasses, *J. Asian Ceram. Soc.* 3 (1) (2015) 116–122.
- [42] H. Bouaamlat, N. Hadi, N. Belghiti, H. Sadki, M. N. Bennani, F. Abdi, T. Lamcharfi, M. Bouachrine, and M. Abarkan, Dielectric Properties, AC Conductivity, and Electric Modulus Analysis of Bulk Ethylcarbazole-Terphenyl, *Adv. Mate. Sc. and Eng.*, (2020), Article ID 8689150, 8 pages. doi:10.1155/2020/8689150.